Proceedings of the 17th World Congress
The International Federation of Automatic Control
Seoul, Korea, July 6-11, 2008

ROBUST CONTROL OF A BENDING-TORSION COUPLED FLEXIBLE ARM WITH UNCERTAINTIES

Toru Watanabe, Ryota Aikawa, Yasuaki Ryokata, and Kazuto Seto

College of Science and Technology, Nihon University
1-8 Kanda-Surugadai, Chiyoda-ku, Tokyo, 101-8308 JAPAN

Abstract: This paper presents a design procedure of H-infinity robust controller of a three-dimensional two links flexible robot arm taking account of posture change and uncertain payload. Two-degree-of freedom model is identified experimentally by utilizing Seto's modeling method. An H-infinity controller is obtained by using a generalized plant including error matrices and two filters; Error matrices represent the fluctuation of parameters between nominal and fluctuated model. Besides, A high-pass and a low-pass filter are introduced to avoid spilover or to realize pseudo-integrator, respectively. The effectiveness of the obtained controller are verified by the simulation and the control experiment.

Keywords: Vibration Control, Robust Control, Flexible Arm, H-infinity Control, Parameter Variation

1. INTRODUCTION

Recently, lightweight robot arms are put into practical use in space development. Such robot arms should have longer arm for wider working space, and should have lighter weight to save launch cost. They make the arm more flexible and consequently need vibration control. In the space arm, one of the main task of such arms is to catch and carry payloads floating in space. The vibration modes may vary according to the variations of angles between links in the practical use. Such variations may arise uncertain vibration modes including bending-torsion coupling that often causes controller instability. Therefore the controller must be designed to possess robust stability against such uncertain coupling.

Many studies concerning bending-torsion coupled vibration of flexible arm has been performed (Matsuno, *et al*., 1997, Ryokata, *et al*., 2006). . . However, most of such studies deal with the case that the bending-torsion coupled vibration modes are supposed to be precisely identified and invariant. As stated before, the vibration modes may vary according to the posture variations of the arm.

In the past, we proposed a design procedure of H-infinity robust controller of the robot arm taking account of posture change, and the effectiveness is verified by the simulation and the control experiment. However, when the mass held in the tip of the arm was increased, the control became unstable. Therefore, the construction of the robust control system against posture change and payload uncertain is requested.

In this research, we propose a design procedure of an H-infinity robust controller of the flexible robot arm taking account of posture change and uncertain payload. Physical model is applied to denote the two links flexible robot arm. Parameters of the model are identified experimentally by utilizing Seto's modeling method. To design robust H-infinity controller, two models are identified. Nominal model case denotes the state that two links are extended straight, while fluctuated model case denotes the state that two links are vertical each other. Robust servo controller design procedure is introduced that applies the H-infinity control theory in consideration of the parameter change due to the posture change and uncertain payload. The effectiveness of the obtained controller are verified by the simulation and the control experiment. Moreover, the obtained controller is compared with the controller that ignores the influence of uncertain payload. Robustness of the controller against to uncertain payload is verified by the control experiment.

2. CONTROL OBJECT

Figure 1 shows a schematic diagram of the two links flexible robot arm introduced as a control object in this research. The two links flexible arm is built by using two actuators and two plates. These plates denote robot arms and are made of thin stainless plates. The entire two links arm has a length of 1110 [mm], a weight of 3200 [g]. Elbow part has a length of 111 [mm], a weight of 1870 [g]. Table 1 shows parameters of each links.

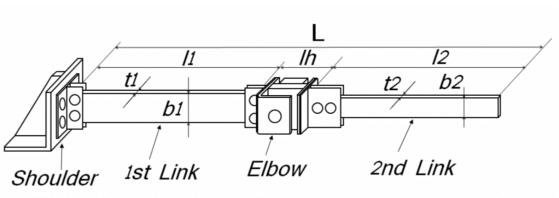

Fig. 1. Schematic diagram of the control object

Table 1 Metrics of the control object

	Length l1 / l2 [mm]	Width b1 / b2 [mm]	Thickness t1 / t2 [mm]	Weight [g]
1st link	600	60	4	1078
2nd link	400	40	2	244

In this research, the physical models were made for two cases respectively; Nominal model case denotes the state that two links are extended straight, while fluctuated model case denotes the state that two links are vertical to each links.

3. MODELING

The dynamics of plate is described as distributed parameter model in general, while lumped parameter model is needed in ordinary H-infinity controller design procedure. In this paper, 2 D.O.F. lumped mass model is introduced and the equivalent parameters of the model are identified by using Seto's modeling method (Seto and Mitsuta, 1991). According to the Seto's method, the maximum amplitude point of each vibration mode should be selected as a "modeling point", where virtual lumped mass to describe equivalent mass of each vibration mode is located.

In this research, mass points are allocated on the elbow and the tip of 2nd link. Figure 2 and Figure 3 show the schematic diagram of lumped mass model for the nominal model and fluctuated model.

Moreover, a physical model was made with the minion of the arm had been made to hold the payload of Fig.4 when a both physical model was made. Payload made of cold-reduced carbon steel (SPCC). The parameters of payload are showed Table 2.

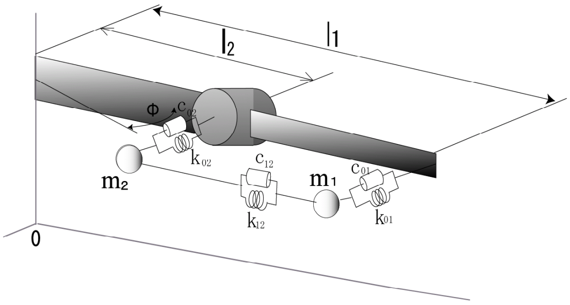

Fig. 2 Schematic diagram of nominal arm model

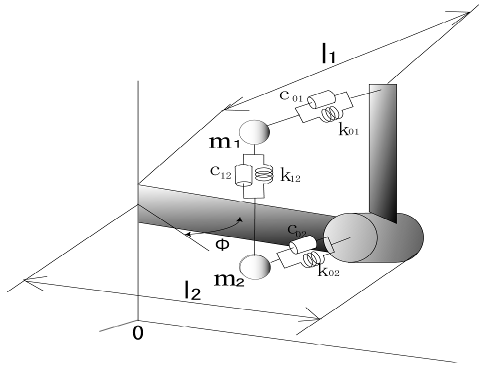

Fig. 3 Schematic diagram of fluctuated arm model

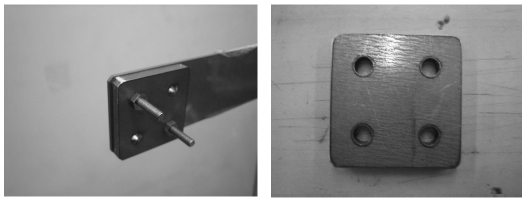

Figure 4. Outlook of payload

Table 2. Identified parameters of the arm

Length [mm]	Width [mm]	Thickness [mm]	Weight [g]
40	40	5.8	77.0

Frequency responses of each model and real arms are shown in Figure 5, respectively. The thick lines denote the responses calculated by using physical models, while the thin lines show the experimental responses, respectively. The input is rotation angle of shoulder actuator and the output is the acceleration at the tip. It is shown that the physical model expresses the vibration characteristic of the arm well.

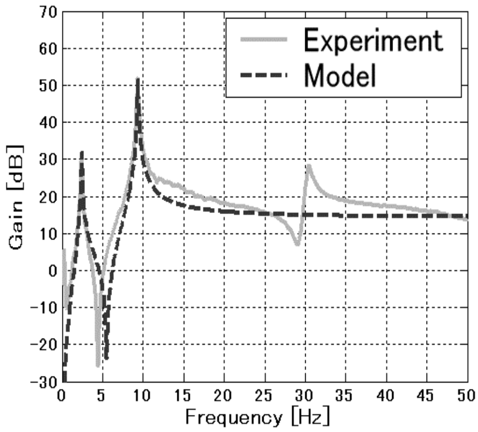

(a) Nominal

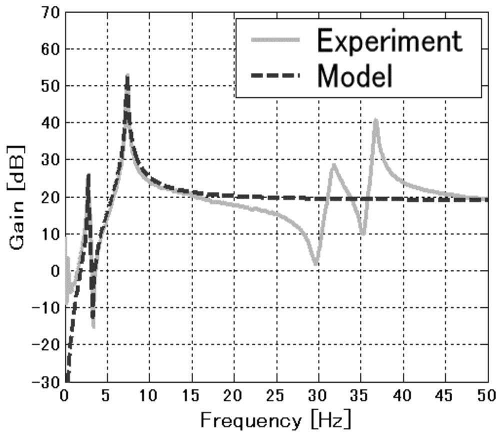

(b) Fluctuated

Fig. 5 Frequency responses of control object

4.CONTROL SYSTEM DESIGN

In this chapter, controller design procedure based on Watanabe and Yoshida's procedure is presented (Watanabe and Yoshida, 1996)

4.1 Expression of structured uncertainties to represent parameter variations

The structured uncertainties represent the fluctuation of parameter between nominal and fluctuated model. The system and output matrix equation with parameter variation can be written as follows;

$$\dot{\mathbf{X}} = (\mathbf{A} + \Delta\mathbf{A})\mathbf{X} + (\mathbf{B} + \Delta\mathbf{B})\mathbf{U} \quad \mathbf{y} = (\mathbf{C} + \Delta\mathbf{C})\mathbf{X} + (\mathbf{D} + \Delta\mathbf{D})\mathbf{U} \tag{1}$$

where ***ΔA, ΔB, ΔC*** and ***ΔD*** denote parameter variations matrices of ***A, B, C*** and ***D*** matrices, respectively. The range of variation of ***A, B, C*** and ***D*** matrices are represented as follows;

$$\Delta\mathbf{A} = \mathbf{A}_{nominal} - \mathbf{A}_{fluctuated} \qquad \Delta\mathbf{B} = \mathbf{B}_{nominal} - \mathbf{B}_{fluctuated}$$
$$\Delta\mathbf{C} = \mathbf{C}_{nominal} - \mathbf{C}_{fluctuated} \qquad \Delta\mathbf{D} = \mathbf{D}_{nominal} - \mathbf{D}_{fluctuated} \tag{2}$$

In the ***ΔA, ΔB, ΔC*** and ***ΔD*** matrices, several rows may contain no value. Such rows are eliminated from ***ΔA, ΔB, ΔC*** and ***ΔD*** matrices to maintain them full rank.

4.2 Shaping low-pass filter and high-pass filter

Figure 6 shows frequency gain characteristic of shaped filters. Broken line denotes the characteristic of high-pass filter to avoid spillover, and bold line denotes that of low-pass filter with integral characteristic to be used as an integrator.
These filters are shaped in frequency domain, transformed into state-space model, and built into generalized plant

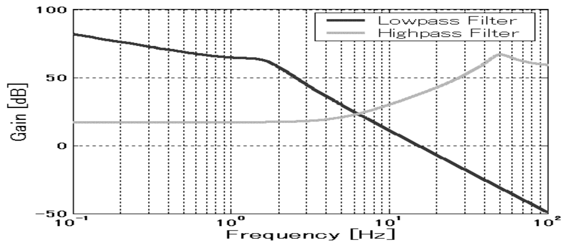

Fig. 6. Frequency characteristics of shaped filters

4.3 Generalized plant

The block diagram of the generalized plant is shown in Fig.7, where $\boldsymbol{A_f}$, $\boldsymbol{B_f}$, $\boldsymbol{C_{p1}}$ are the ***A, B*** and ***C*** of state equation (2) with nominal model respectively, $\boldsymbol{X_c}$ and ***u*** denote ***X*** and ***U*** in equation (2) respectively, w_a, w_b w_c, and w_{se}, w_{sp} are fictitious disturbance input, and Z_1, Z_2, Z_3, Z_{se} and Z_{sp} are the performance index associated with the H∞ constraint, respectively. The observed outputs are transverse acceleration at the mass point 1 and the angle of the rotation of shoulder actuator. The feedback controller ***K*** is sought by applying H∞ control theory account of the generalized plant. The generalized plant can be written as follows;
X, Z and ***W*** denotes the state vector, disturbance input vector and performance index vector of the generalized plant, and $\boldsymbol{A_{1z}}$, $\boldsymbol{B_{1z}}$, $\boldsymbol{B_{2z}}$, $\boldsymbol{C_{1z}}$, $\boldsymbol{C_{2z}}$, $\boldsymbol{D_{11z}}$, $\boldsymbol{D_{12z}}$, $\boldsymbol{D_{21z}}$ and $\boldsymbol{D_{22z}}$ are state, input, output and disturbance matrices of the generalized plant, respectively. I (with suffix) denotes unit matrix, and bf denotes observation noise input matrix. The CACSD software MATLAB is applied for numerical calculation to obtain a controller. The performance of the obtained controller is examined through computer simulation before experiment.

$$\begin{aligned} \dot{\mathbf{X}} &= \mathbf{A}_{1z}\mathbf{X} + \mathbf{B}_{1z}\mathbf{W} + \mathbf{B}_{2z}\mathrm{u} \\ \mathbf{Z} &= \mathbf{C}_{1z}\mathbf{X} + \mathbf{D}_{11z}\mathbf{W} + \mathbf{D}_{12z}\mathrm{u} \\ \mathbf{Y} &= \mathbf{C}_{2z}\mathbf{X} + \mathbf{D}_{21z}\mathbf{W} + \mathbf{D}_{22z}\mathrm{u} \end{aligned} \tag{3}$$

where

$$\mathbf{X} = \begin{bmatrix}\mathbf{X}_f & \mathbf{X}_{sp} & \mathbf{X}_{se}\end{bmatrix}^T$$
$$\mathbf{W} = \begin{bmatrix}\mathbf{W}_a & \mathbf{W}_b & \mathbf{W}_c & \mathbf{W}_d & \mathbf{W}_{sp} & \mathbf{W}_{se} & \mathrm{r}\end{bmatrix}^T$$

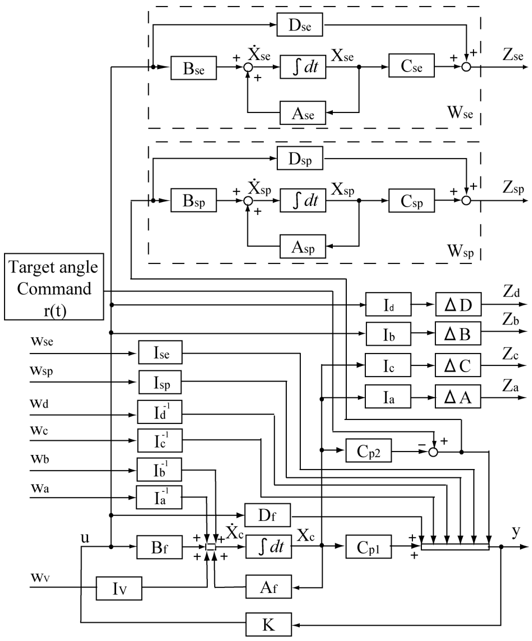

Fig.7. Schematic diagram of the generalized plant

5.EXPERIMENTAL SET-UP

Figure 8 shows the experimental set-up for the flexible arm. The measured outputs are the transverse acceleration to the mass point 1(tip of the 2nd link) measured by using an acceleration pickup, and the angle of the rotation of shoulder actuator measured by using a potentiometer. The measured values are sent to personal computer through the 16-bit A-D board. The personal computer calculates control input according to obtained controller. The control input is sent to a servo-driver though 16-bit D-A board that drives servomotor to control. In this paper, the elbow actuator is used only to change the posture of the arm, not to suppress vibration.

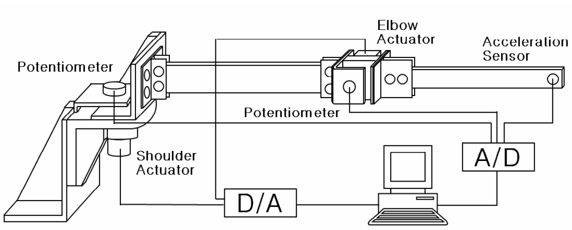

Figure 8. Experimental setup

6.EXPERIMENTAL RESULT

The robot arm is holding the payload of 77.0 [g]. Figure 9 and 10 shows experimental results of nominal posture and fluctuated posture. Figures (a) show time response of the angle of shoulder actuator with ordinary proportional controller (P-controller), and obtained H-infinity controller subjected to target rotation 30 [deg]. Figures(b) show time responses of acceleration at mass point 1 (at the tip of 2nd link).

Figure 9-(a) and 10-(a) clearly indicates that the H-infinity controller achieves as high tracing control performance as

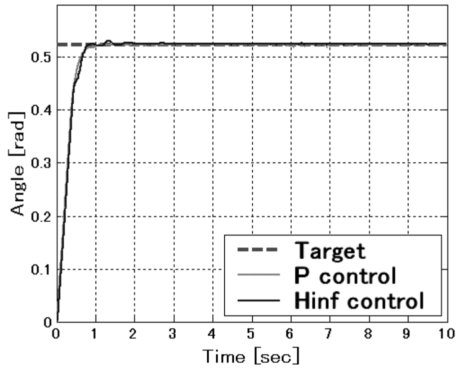

(a) Rotation angle of the shoulder

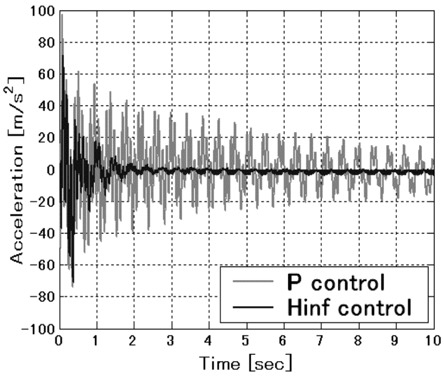

(b) Acceleration at the tip of the arm
Fig.9 Nominal posture with Payload 77.5g

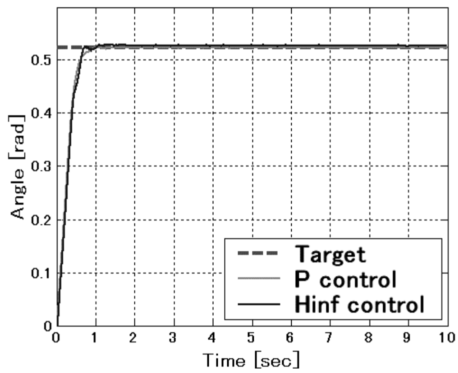

(a) Rotation angle of the shoulder

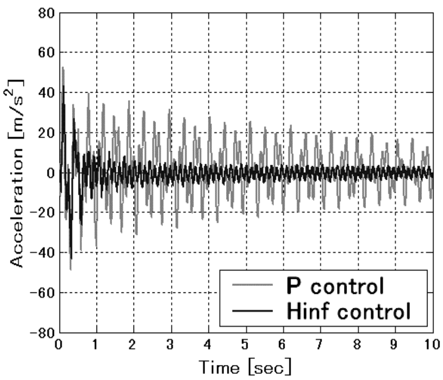

(b) Acceleration at the tip of the arm
Fig.10 Fluctuated posture with Payload 77.5g

P-controller. The gain of P-controller is tuned experimentally for comparison.
Figure 9-(b) and 10-(b) clearly indicate that the H-infinity controller achieves higher damping effect than P-controller. These figures indicate that H-infinity controller possesses robust vibration control performance against posture change and holding payload.
In addition, robustness to the uncertain payload is verified. Figure 11 and 12 show the control experimental results of the arm holding payload of 369.3 [g]. Figure 11-(a) and 12-(a) clearly indicates that the H-infinity controller achieves as high tracing control performance as P-controller. Figure 11-(b) and 12-(b) clearly indicate that the H-infinity controller achieves higher damping than P-controller.

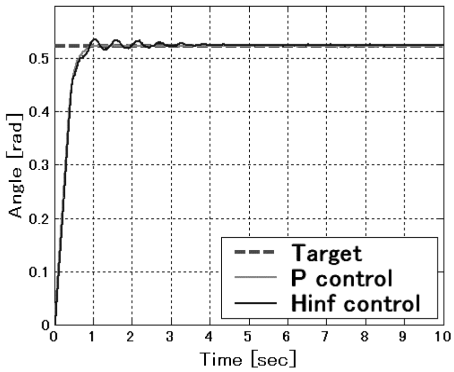

(a) Rotation angle of the shoulder

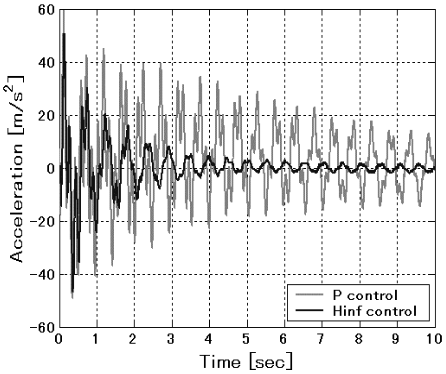

(b) Acceleration at the tip of the arm
Fig.11 Nominal posture with Payload 369.3g

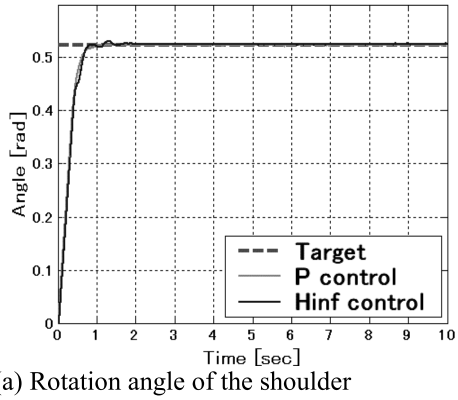

(a) Rotation angle of the shoulder

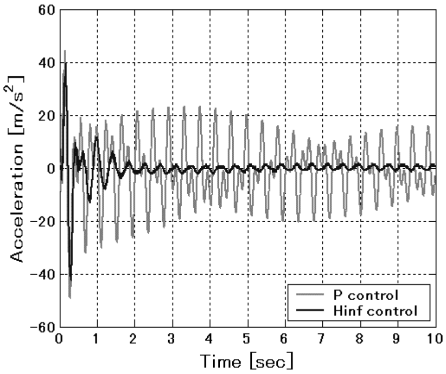

(b) Acceleration at the tip of the arm
Fig.12 Fluctuated posture with payload 369.3g

Besides, Figure 13 shows a time response of tip acceleration when control experiment is carried out with a controller designed under almost the same condition as shown above. The only difference is that the controller is designed taking account of posture change only. The controller is applied to the arm in fluctuated posture with payload 369.5g. It is clearly shown that the controller possess instability due to unmodeled payload. It was confirmed that the robustness of the controller against uncertain payload was expanded by taking account of the weight of the holding payload.

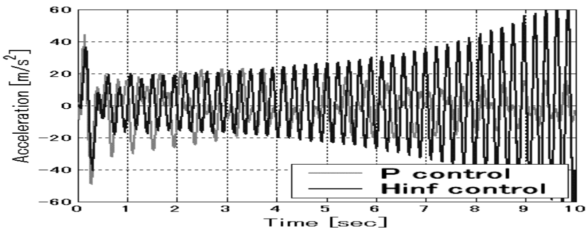

Fig.13 Tip acceleration of the arm in fluctuated posture with payload 369.3g controlled by previous controller without consideration for payloads.

7. CONCLUSIONS

In this paper, robust motion and vibration control of two links flexible robot arm is dealt with. A design procedure is presented that integrates modeling and H-infinity controller design procedure taking account of model error due to posture change and uncertain payload. The obtained H-infinity controller achieved good control performance and robustness to uncertain payload simultaneously. According to these results, the presented controller design method is certified to be effective.

REFERENCES

Matsuno, F., Umeyama,, S., Kasai, S. and Kanzawa., T. (1997), Robust Bending and Torsional Vibrations and Contact Force Control of a Flexible Arm, Vibrations of a Flexible Arm, *Transactions of the Society of Instrument and Control Engineers*, **Vol.33, No.7**, pp.674-679.(In Japanese)

Ryokata, Y. Nakagawa, K. Watanabe, T. and Seto, K (2006) H-infinity Robust Servo Motion and Vibration Control of Two Links Flexible Robot Arm in Consideration to Variations of Posture, *8th International Conference on Motion and Vibration Control (Movic2006)*, pp766-771.

Seto, K. and Mitsuta. S. (1991) A New Method for Making a Reduced-order Model of Flexible Structures Using Unobservability and Uncontrollability and Its Application in Vibration Control, *Transactions of the Japan Society of Mechanical Engineers, Series C,* **Vol.57, No.542**, pp.3393-3399. .(In Japanese)

Watanabe, T. and Yoshida., K. (1996) Robust Vibration Control of a Flexible Structure Taking Account of Parameter Variations and Model Errors in Uncontrolled Modes, *Transactions of the Society of Instrument and Control Engineers*, **Vol.32, No.7**, pp.1001-1010. .(In Japanese)